Supplementary Information for

Targeting Mitochondria Degradation by Chimeric Autophagy-Tethering Compounds

Zhenqi Liu,[†,‡] Geng Qin,[†,‡] Jie Yang,[†,‡] Wenjie Wang,[†,‡] Wenting Zhang,[†,‡] Boxun Lu,[,#] Jinsong Ren,[†,‡] and Xiaogang Qu*[†,‡]*

[†]Laboratory of Chemical Biology and State Key Laboratory of Rare Earth Resource Utilization, Changchun Institute of Applied Chemistry, Chinese Academy of Sciences, Changchun, Jilin 130022, China.

[‡]School of Applied Chemistry and Engineering, University of Science and Technology of China, Hefei, Anhui 230026, China.

[#]Neurology Department at Huashan Hospital, State Key Laboratory of Medical Neurobiology, and Ministry of Education Frontiers Center for Brain Science, School of Life Sciences, Fudan University, Shanghai, China.

This PDF file includes:

Chemicals and Antibodies

Scheme 1 was draw by Figdraw (ID: TYTIY8088b). 3-oxo-3-phenylpropionate, 1,3,5-trihydroxybenzene, 6-Iodo-1-hexyne, and (3-bromopropyl) triphenyl phosphonium bromide were purchased from Energy Chemical (shanghai, China). Hoechst 33342 (abs813337) and Crystal violet (abs47047863) were purchased from Absin (shanghai, China). 3-(4, 5-dimethyl-2-yl)-2, 5-diphenyltetrazolium bromide (MTT) was purchased from Sangon Biotechnology Inc. (Shanghai, China). Rapamycin and 3-methyladenine (3-MA) were purchased from Sparkjade Biotechnology. The following primary antibodies were used in assays: anti-HSP60 (Beyotime, AF0186), anti-TOMM20 (Beyotime, AF1717), anti-PDI (Beyotime, AF0264), anti-LC3A/B Mouse mAb (absin, abs158317, 1:100 dilutio), and anti-β-actin (Bioss, bs-0061R). Secondary antibodies for immunoblotting were: anti-mouse IgG, HRP-linked antibody (Sangon Biotech, D110098), anti-rabbit IgG, HRP-linked antibody (Sangon Biotech, D110065). Secondary antibodies used in immunofluorescence assay was: FITC-labeled Goat Anti-Rabbit IgG (H+L) (Beyotime, A0562). Cy3-conjugated Goat anti-Rabbit IgG (Sangon Biotech., D110062), FITC-conjugated Goat anti-mouse IgG (Sangon Biotech., D110105).

Measurements and characterizations

The Liquid Chromatography Mass Spectra (LCMS) was obtained using Quattro Premier XE (USA). The confocal laser scanning microscopy (CLSM) characterization was acquired by a top-of-the-line motorized upright (Nikon Eclipse Ni-E, Japan).

Cells and culture conditions.

Human breast cancer cell line MCF-7; human malignant melanoma cell line A375; human pancreatic carcinoma cell line Panc-1; human cervical cancer cell line HeLa; human glioblastoma cell line U87-MG; human hepatocellular carcinoma cell line HepG2; mouse connective tissue established cell line L929; and human embryonic kidney 293T cell line were cultured in Dulbecco's Modified Eagle Medium (DMEM) supplemented with 10% FBS, 100 IU penicillin and 100 mg/ml streptomycin. Human breast cancer cell line MDA-MB-231; human erythroleukemic cell line K562; and mouse melanoma cell line B16 were maintained in RPMI-1640 supplemented with 10% FBS, 100 IU penicillin and 100 mg/ml streptomycin.

Isolation of mitochondria

MCF-7 cells were grown to ~90% confluency in 15-cm plates. Cells were then harvested by trypsinization, pelleted, and washed in PBS. Mitochondria were isolated using the Cell Mitochondria Isolation Kit (Beyotime, C3601) according to the manufacturer's instructions. Protein concentrations of mitochondrial were measured by BCA assay.

Analysis of the effects of mitophagy inducers on mitochondrial function

To analyze the effects of different mitophagy chemical inducers on mitochondrial membrane potential (MMP) *in vitro*, isolated mitochondria were stained with TMRE

(Beyotime, C2001S) in mitochondria storage buffer for 20 minutes at 37°C, followed by 3 washes. Isolated mitochondria were resuspended in mitochondria storage buffer in the CLARIOstar ^{plus} microplate readers for 30 min to allow stabilization. 100 X working solution of different mitophagy inducers was then added to desired wells. Subsequently, the MMP of isolated mitochondria were detected in CLARIOstar ^{plus} microplate readers for another 6 hours. The samples lacking mitophagy inducers were treated with 1% DMSO as a vehicle control. The final concentrations of mitophagy inducers were as follows: FCCP, 10 μM; mito-ATTECs, 20 and 30 μM.

Confocal Laser Scanning Microscopy analysis: For mitochondrial localization determination, Mitotracker Red CMXRos (MTR, Beyotime, C1035) staining was used after mito-ATTEC treatment. After that, cells were stained with 100 nM MTR in HBSS (Hank's Balanced Salt Solution, Servicebio) for 20 minutes, followed by 3 washes with PBS. Images were taken on confocal microscopy (Nikon Eclipse Ni-E, Japan) under the same parameters. Co-localization between mito-ATTEC and Mito-Tracker Red was analyzed by ImageJ.
The MMP was detected by JC-1 dye (10 μg/ml, Solarbio, J8030). The cellular ROS content was detected by DCFH-DA dye (Beyotime, S0033S).
MTR dye was used to evaluate the mitochondrial mass. Cells were stained with MTR dye (100 nM) for 20 min at 37°C. Excess probe was removed by washing. Then the cells were incubated with mito-ATTEC in the condition as mentioned in article. The MTR fluorescence level was counted from at least 200 cells using ImageJ.
In order to quantitatively analyze the colocalization of mitochondria and lysosomes, MTR staining was used before mito-ATTEC treatment as mentioned. After that, the cells were treated with mito-ATTECs and then stained with Lyso-Tracker Green (Beyotime, C10475). Co-localization between mitochondria and lysosomes was analyzed by ImageJ.
For immunofluorescence assay, cells were treated with mito-ATTECs as mentioned in article, then fixed and blocked by 5% BSA in PBS solution. After that, the cells were incubated with primary antibodies (anti-TOM20,AF1717, 1:200 dilution; anti-LC3A/B Mouse mAb, abs158317, 1:200 dilution) at 4°C overnight. Then, the cells were washed and incubated with appropriate secondary antibodies for 2 h at room temperature. The mitochondria-LC3 co-localization was detected at 6 h post-treatment.

Determination of mtDNA content: Genomic DNA of cells was extracted using the SPARKclassic Genomic DNA Kit (Shandong Sparkjade Biotechnology Co., Ltd., AA0901-A). The mtDNA content was determined by qPCR assay. The relative changes of mtDNA was determined by normalizing to GAPDH.

Reagents, siRNAs and Transfections: siRNAs against Atg5 was purchased from RiboBio Co., Ltd (Guangzhou, China), and they were used for transfections with Oligofectamine for 48 hour. Non-targeting scrambled siRNAs (RiboBio Co., Ltd) were used as controls. GAPDH were used as internal controls. human ATG5_siRNA, 5′-GCCUGUAUGUACUGCUUUA-3′. Efficiency of siRNAs was evaluated by western

blotting.

Cytotoxicity Studies.
Cell viability was measured by MTT assays. Cells were seeded at a density of 5000 cells/well on 96-well plates. After 24 h incubation, cells were treated under different conditions and then MTT assays were carried out. To determine toxicity, 10 μL of MTT solution was added to each well and the cells were incubated for 4 h. After adding 100 μL DMSO, the absorbance of formazan was read at 570 nm on a SpectraMax M5 microplate reader. Three replicates were done for each treatment group.

Transwell invasion assay.
Boyden chamber transwell pre-coated with growth factor-reduced Matrigel Matrix were purchased from Fisher Scientific. Transwell invasion assays were performed according to the manufacturer's protocol. Briefly, 5×10^5 MCF-7 cells were seeded into each transwell, filled with serum-free culture medium. The bottom wells were filled with cell culture medium with 10% FBS and mito-ATTECs. After 48 h, cells were fixed with 10% formalin and stained with 5% crystal violet in 70% ethanol. Invaded cells were counted at a magnification of 10 × in three randomly selected areas of each transwell, and the results were normalized to the control.

Western blotting analysis
MCF-7 cells were seeded in 24-well culture plates. At 60% confluence, the cells were incubated with mito-ATTECs in the condition as mentioned in article. Cells were rinsed with PBS and lysed with RIPA buffer (Bioss, C5029) supplemented with PMSF (Bioss, D10411) on ice for 30 min. The cells were scraped and centrifuged at 15,000g for 15 min at 4 °C. The supernatant was collected and the protein concentration was determined by BCA kit. Denatured cellular extracts were resolved by 12% SDS–polyacrylamide gels and then transferred to a PVDF membrane. Blots were blocked in TBS buffer containing 5% (wt/v) non-fat milk, washed three times with TBS with 0.1% Tween-20 (TBST), and incubated with primary antibodies overnight at 4 °C and then incubated with appropriate secondary antibodies for another hour at room temperature. After washing with TBST, protein bands were visualized with ECL Western Blotting Substrate (Solarbio, PE0010).
The following antibodies were used: anti-HSP60 (Beyotime, AF0186, 1:1000 dilution), anti-TOM20 (Beyotime, AF1717, 1:1000 dilution), anti-PDI (Beyotime, AF0264, 1:1000 dilution), and anti-β-actin (Bioss, bs-0061R, 1:1000 dilution).

Measurement of ATP.
ATP levels were quantified using the Enhanced ATP Assay Kit (Beyotime, S0027), as described by the manufacturer.

Mito-Keima mitophagy assay
Keima is a pH-sensitive, dual-excitation fluorescent protein that also exhibits resistance to lysosomal proteases. Under normal growth conditions (pH 8.0), the shorter-wavelength excitation predominates. Within the acidic lysosome (pH 4.5) after

mitophagy, mt-Keima undergoes a gradual shift to longer-wavelength excitation. Dual-excitation imaging in MCF-7 cells were down with two sequential excitation lasers (488 and 561 nm) in combination with a 570–620-nm emission range. we chose to depict the mito-Keima fluorescence signal from 561-nm laser excitation (acidic) in red and the signal from 458-nm laser excitation (neutral pH) in green
MCF-7 cells were infected with lentivirus containing mito-Keima vector and grown for 3 days. MCF-7 cells stably expressing mito-Keima under different conditions were imaged by Nikon confocal microscope. Our laser sources for CLSM were 488 and 561 nm rather than the 458 and 561 nm, resulting in some overlap of the ‘‘red’’ signal into the ‘‘green’’ images.

Ultrastructure analysis by TEM.
Cells grown in the absence or presence of mito-ATTEC were fixed in 2.5% glutaraldehyde (w/v) in 0.1 M cacodylate following removal of culture medium. After postfixation in 2% (v/v) osmium tetroxide, specimens were embedded in Epon 812, and sections were cut orthogonally to the cell monolayer with a diamond knife. Thin sections were visualized in a JEOL 1010 transmission electron microscope.

Animal experiments.
The C57BL/6 mice were purchased from Jilin University and acclimatized for 1 week before experiments. All animal experiments and maintenance protocols were complied with the Institutional Animal Care and Use Committee of Jilin University.

Measurement of xenograft-driven tumor growth *in vivo*.
The subcutaneous xenograft B16 tumor model was established in the C57BL/6 mice. The mice were randomly divided into three groups (n = 5), and the B16 cells (2×10^6) were injected subcutaneously. After tumors reached to 100-150 mm^3 volume, animals in each group were treated for 14 days: (1) DMSO vehicle; (2) precursors in DMSO vehicle; (3) mito-ATTEC in DMSO vehicle. Compounds were administered into the lateral tail vein every two days. We determined 17 mg/kg as a suitable injection dose, which can reach ~ 12 μM in the tumor tissues after injection. The body weight and tumor volume were quantified every two days after administration.

The formation of melanoma in lung and liver.
B16F10 cells were injected into the lateral tail vein of C57BL/6J mice (5×10^5 cells/per mouse). Three days after inoculation, mice were divided into DMSO vehicle and mito-ATTEC-treated groups (n = 6). The treatments were done by tail vein injection every two days. The mice were sacrificed 14 days after mito-ATTEC treatment.

Mitophagy assessment *in vivo* by western blot.
Tumor tissue lysates were prepared according to manufacturer’s instructions (Beyotime, P0013F). Following centrifugation to remove insoluble material, protein levels in soluble lysates were quantified using BCA assays (Beyotime, P0010). Denatured cellular extracts (15 μg/lane) were loaded onto 12% SDS–polyacrylamide gels.

Immunoblotting was performed as described for the cell lines.

H&E staining.
The major organs (heart, liver, spleen, lung, and kidney) of the melanoma-bearing mice in the above three groups were collected, and fixed with neutral buffered formalin. Then the organs were embedded into paraffin and sectioned into 4 μm thickness for H&E staining. The images of these sections were taken using a microscope under bright field.

The biocompatibility of mito-ATTECs in C57BL/6J mice
Healthy C57BL/6J mice were randomly divided into three groups. The mice in control group and experimental group were intravenously injected with PBS and mito-ATTECs (17 mg/kg or 34 mg/kg), respectively. Within 21 days after injection, the weight of mice was measured every 3 days. After 21 days treatment, blood samples of the mice were collected for whole blood panel analysis and serum biochemical analysis. The blood biochemistry markers (WBC, RBC, MCV, HCT, MCH, MCHC, PLT and HGB) and liver function markers (ALT, ALP, ALB, AST, and TP) were tested.

Statistical analysis.
All of the data were presented as the mean ± standard deviation (SD). All figures were obtained from a minimum of three independent experiments. Statistical evaluation was performed using two-tailed Student's t test analysis. Asterisks indicated significant differences (*$P < 0.01$, **$P < 0.005$, ***$P < 0.001$).

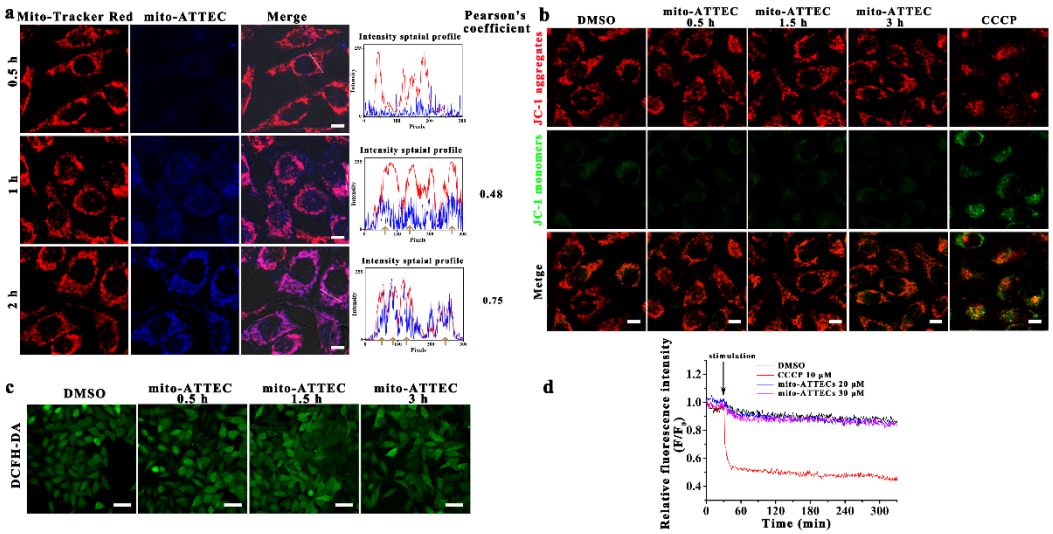

Figure S1. Targeting mito-ATTECs to mitochondria did not alter mitochondrial function or disrupt mitochondrial integrity. (a). Mito-ATTECs (30 μM) displayed obvious colocalization with mitochondria within 2 h, which suggested effective cell penetration and mitochondria accumulation of mito-ATTEC molecules. Co-localization between mito-ATTECs (blue) and Mito-Tracker Red (red) was analyzed by ImageJ. scale bar, 10 μm. (b). Representative images of mitochondrial membrane potential (MMP) using JC-1 probe. Compared to CCCP (10 μM, 1 h), mito-ATTECs treatment (30 μM) had no notable adverse effects on mitochondrial MMP. Scale bars, 10 μm. (c). Representative images of cellular ROS levels using DCFH-DA probe. ROS levels in the mito-ATTEC-treated cells (30 μM) were similar to those in DMSO-treated cells. Scale bars, 50 μm. (d). To analyze the effects of different mitophagy chemical inducers on MMP *in vitro*, isolated mitochondria were stained with TMRE. After 30 min incubation, 100 X working solution of mitophagy inducers (CCCP or mito-ATTECs) was then added to desired wells. Subsequently, the MMP of isolated mitochondria were detected in CLARIOstar ^{plus} microplate readers for another 6 hours. CCCP induced mitochondrial membrane depolarization, whereas mito-ATTEC did not disrupt mitochondrial integrity. All data are representative of at least three independent biological replicates.

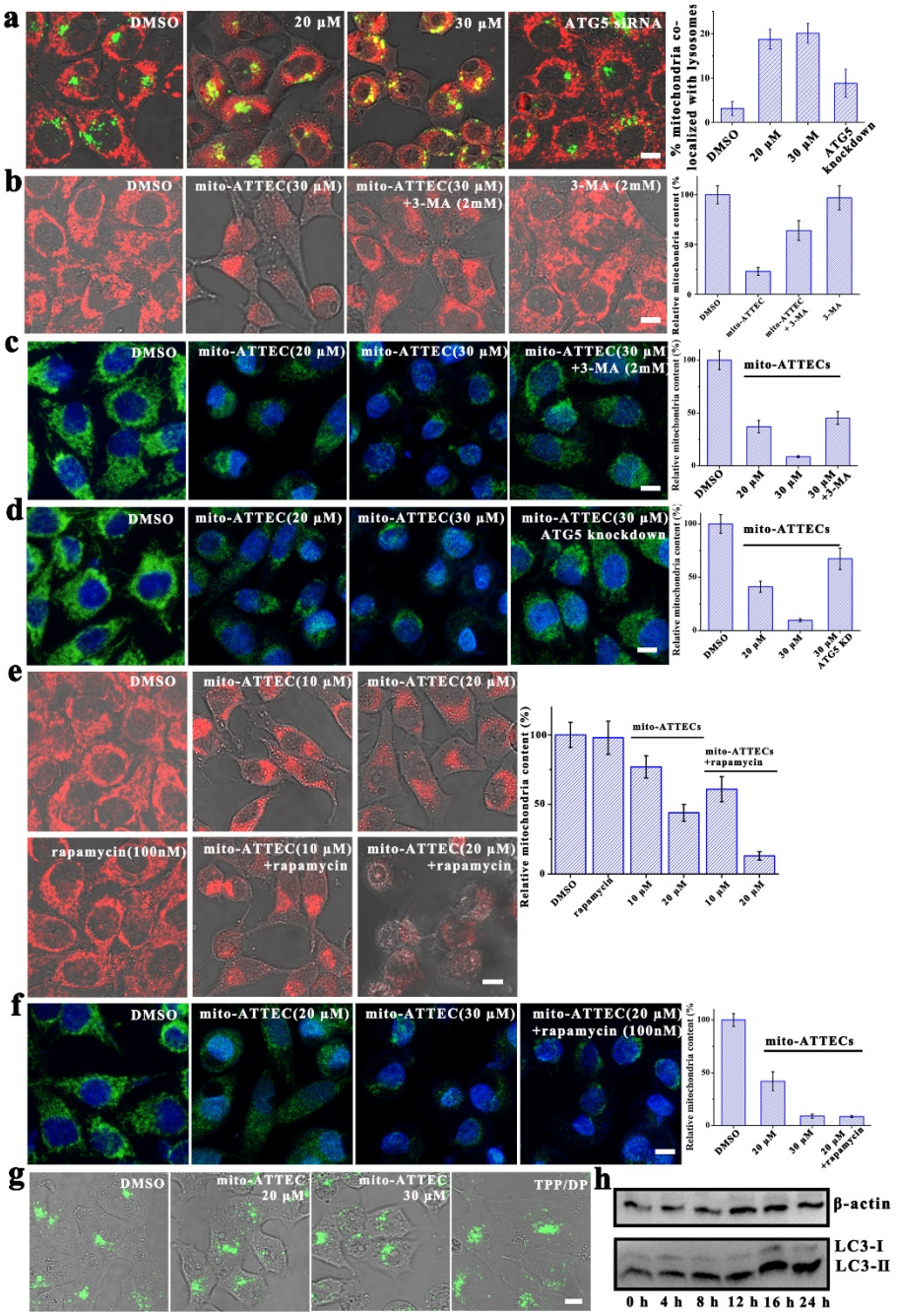

Figure S2. Mito-ATTECs target mitochondria to autophagosomes for degradation**.** Scale bars, 10 μm. (a). Mito-ATTECs treatment (20 μM or 30 μM, 12 h) induced partial colocalizations of mitochondria (MitoTracker, Red) and lysosomes (LysoTracker, green). The percentage of mitochondria that were colocalized with lysosomes was analyzed by Nikon colocalization software and shown in right. (b and c). Co-treatment with 3-MA (2 mM) partially blocked mito-ATTEC-induced mitochondrial depletion. Mitochondrial levels were determined by MTR dye (b) or TOM20 (c) immunofluorescence assay. Values were expressed as percentages in comparison with the DMSO-treated group (set to 100%). (d). Knockdown of ATG5 also abolished mito-ATTECs-mediated mitochondrial depletion. Mitochondrial levels were determined by TOM20 immunofluorescence assay. (e and f). Autophagy activation by rapamycin (100 nM) sensitized MCF-7 cells to mito-ATTEC-induced mitochondrial depletion. Cellular mitochondrial levels were determined by MTR dye (e) or TOM20 (f) immunofluorescence assay. (g). Representative images of lysosomes using Lysotracker

Green. Mito-ATTECs treatment (20 μM or 30 μM, 12 h) did not change the lysotracker puncta number, suggesting no influence on lysosomes. (h). Representative images of LC3B western blots of MCF-7 cells treated with the mito-ATTECs (20 μM). No significant effects (LC3-II/β-actin) by treatment of mito-ATTECs (0h, 4h, 8h, 12h, 16h or 24h at 20 μM) were observed.

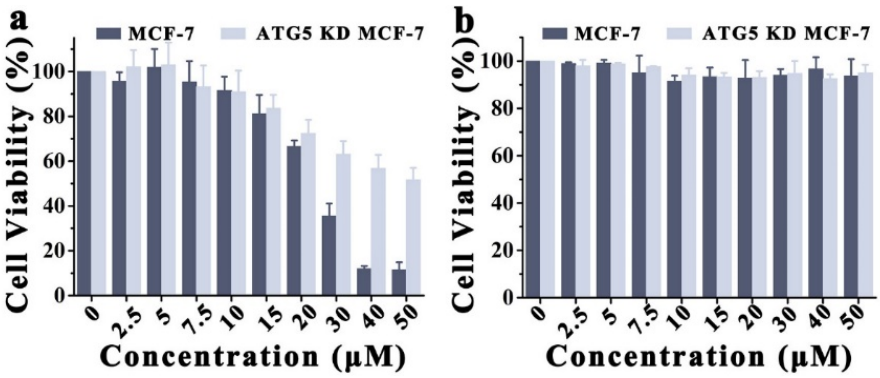

Figure S3. Knockdown of ATG5 protected MCF-7 cells from mito-ATTECs-induced cell death. (a). Cytotoxicity of mito-ATTECs on MCF-7 cells or ATG5 KD MCF-7 cells (ATG5 knockdown). (b). Cytotoxicity of precursors (alk-DP and azi-TPP) on MCF-7 cells or ATG5 KD MCF-7 cells. Data were presented as mean ± SD (n = 3 independent experiments).

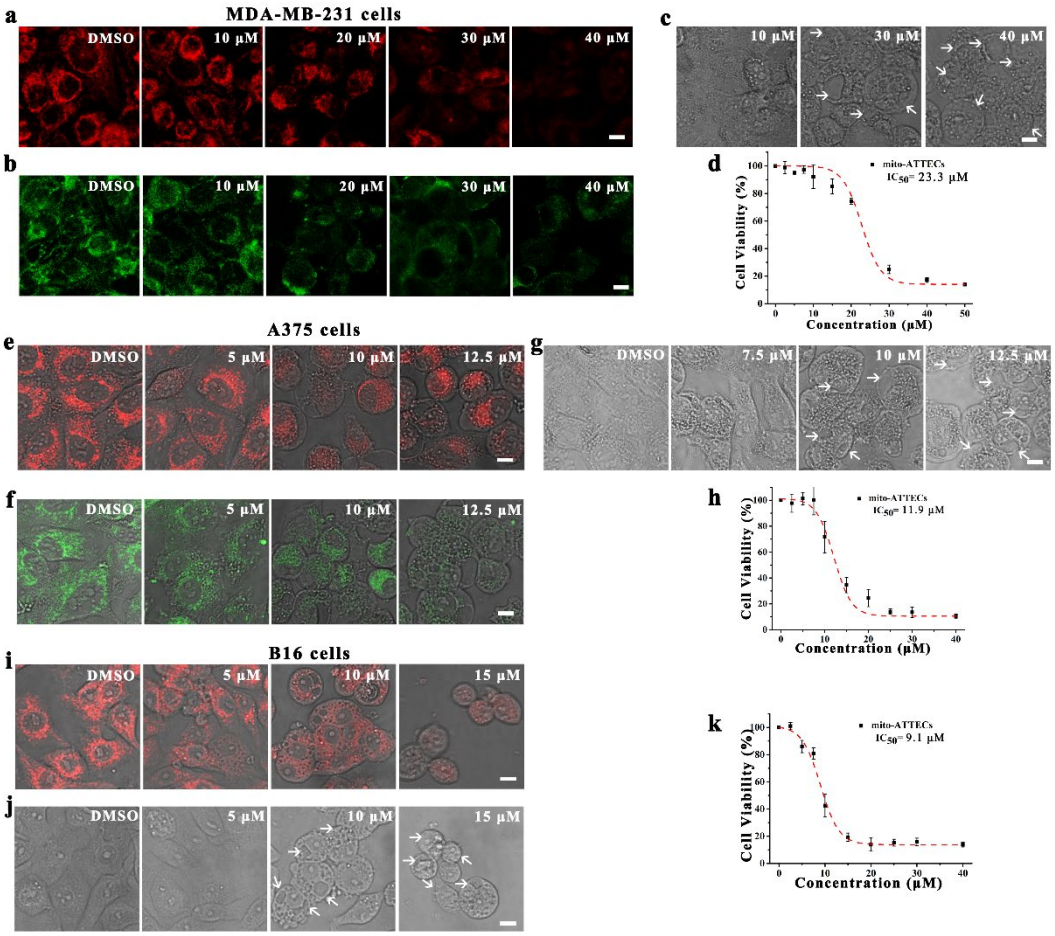

Figure S4. Broad activity of mito-ATTEC against tumor cell lines. Scale bars, 10 μm. (a-d). Mito-ATTEC treatment leads to mitochondrial depletion and autophagic cell death in MDA-MB-231 cells. Mitochondrial levels were determined by MTR dye (a) or TOM20 (b) immunofluorescence assay. Moreover, mito-ATTEC induced autophagic cell death in MDA-MB-231 cells. Arrows indicated autophagic vacuoles in bright field images of mito-ATTEC-treated cells. Cytotoxicity of mito-ATTECs on MDA-MB-231 cells was evaluated by MTT assay (d). Data were presented as mean ± SD (n = 3 independent experiments). Similarly, mito-ATTEC treatment leads to mitochondrial depletion and autophagic cell death in both A375 cells (e-h) and B16F10 cells (i-k).

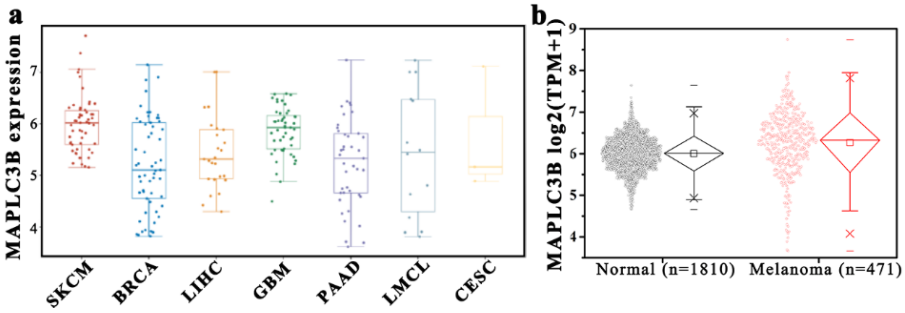

Figure S5. (a). LC3B expression in several tumor cell lines. SMCM: skin cutaneous melanoma; BRCA: breast invasive carcinoma; LIHC: Liver hepatocellular carcinoma; GBM: Glioblastoma multiforme; PAAD: pancreatic adenocarcinoma; LCML: chronic myelocytic leukemia; CESC: Cervical squamous cell carcinoma and endocervical adenocarcinoma. (b). LC3B expression in melanoma and normal tissues.

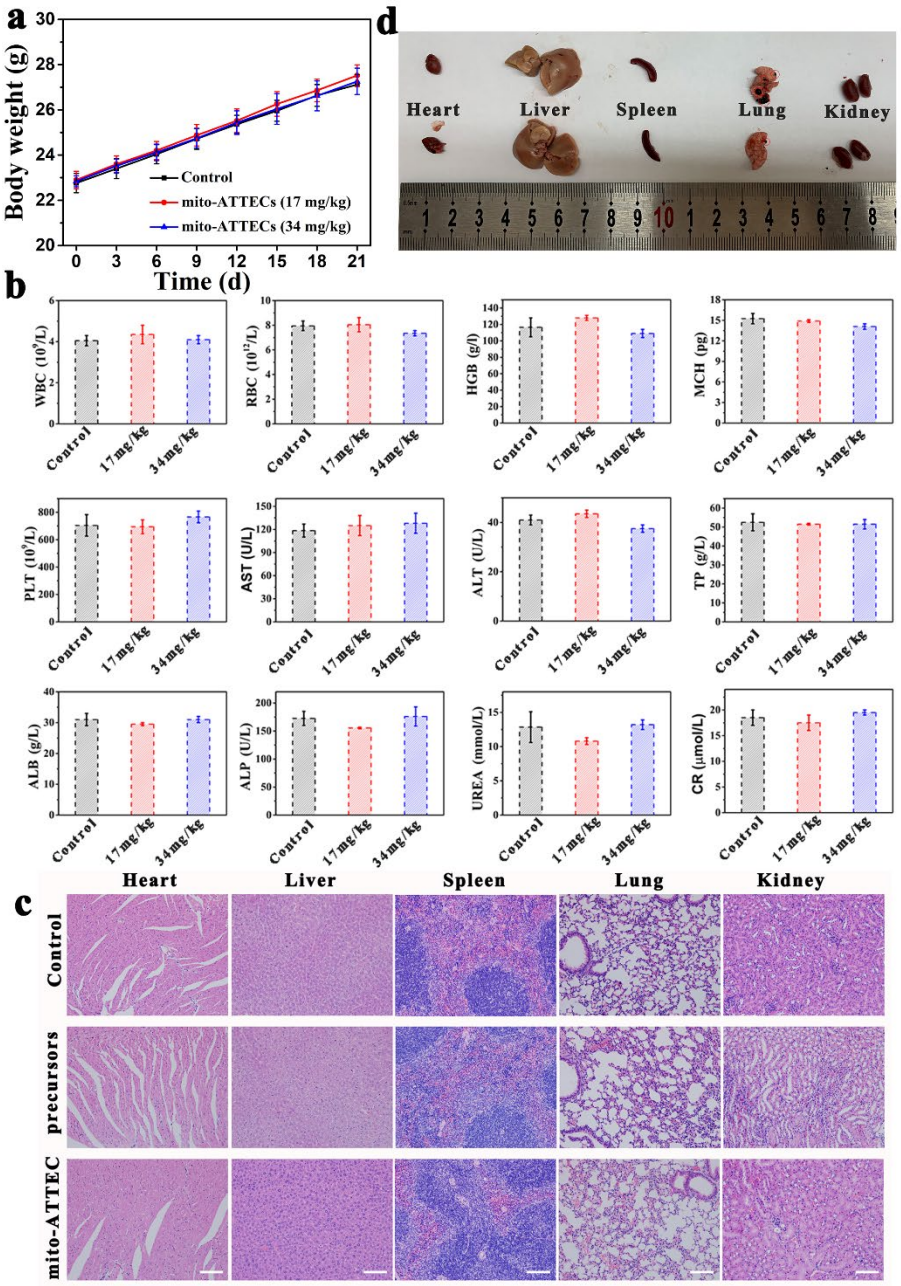

Figure S6. *In vivo* evaluation on the anti-melanoma activity. (a-b). 3-week toxicology study of mito-ATTECs (17 mg/kg or 34 mg/kg) was conducted in C57BL/6J mice. The body weight changes of C57BL/6J mice after different treatment (a). The hematological parameters and blood biochemical levels of the C57BL/6J mice after different treatment (b). (c). Representative images of H&E-stained slices from subcutaneous melanoma-bearing mice after different treatment. Scale bars, 100 μm. (d). Mito-ATTECs (17 mg/kg) inhibited the formation of tumors in lung in C57BL/6J mice. B16F10 cells were injected into the lateral tail vein of C57BL/6J mice (n = 5). Mito-ATTECs were administered 3 d after inoculation.

Preparation of DP (5,7-dihydroxy-4-phenyl-2H-chromen-2-one) MS m/z (ESI): 255.1 $[M+H]^+$.

Add ethyl 3-oxo-3-phenylpropionate (1.5 g, 7.82 mmol) and 1,3,5-trihydroxybenzene (0.99 g, 7.82 mmol) to the reaction flask, add 10 mL of trifluoro acetic acid, stirred at room temperature for 16 hours. After the reaction was completed, water (70 mL) was added, the product was filtered. The obtained solid was purified by reverse phase chromatography to obtain a yellow solid (1 g, yield: 39.8%).

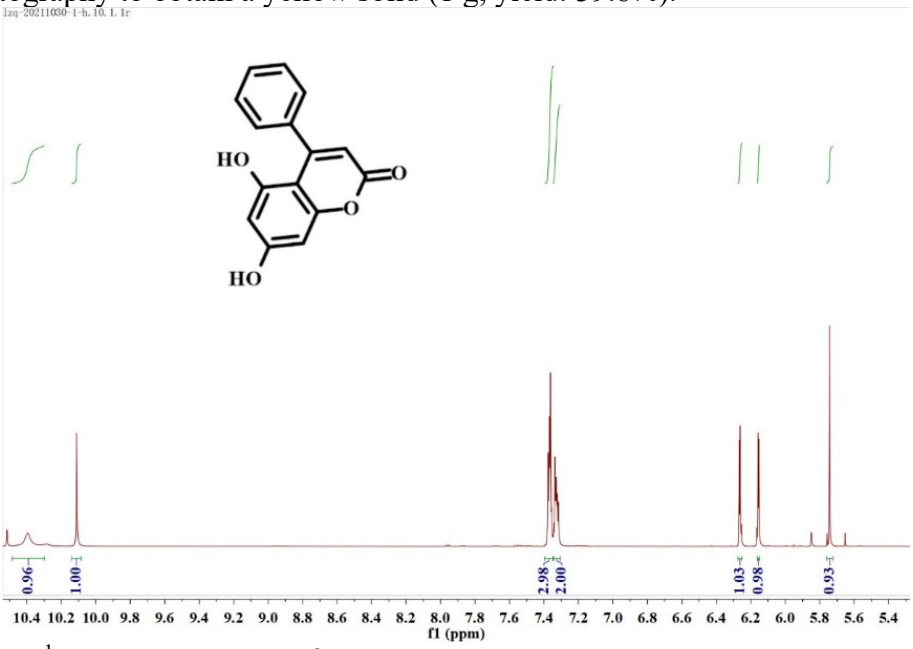

Figure S7. ^{1}H NMR spectrum of DP.

Preparation of alk-DP MS m/z (ESI): 335.1 $[M+H]^+$

Add 6-Iodo-1-hexyne (81.1 mg, 0.39 mmol), DP (992 mg, 0.39 mmol), potassium carbonate (161.8 mg, 1.17 mmol) and potassium iodide (16.6 mg, 0.1 mmol) to a 10 mL flask and add DMF (2 mL), stirred at 60°C for 18 hours. The reaction was cooled to room temperature, water (15 mL) was added, and extracted with ethyl acetate (4x15 mL). The organic layer was combined and spin-dried, and the resulting product was purified by reverse phase chromatography to obtain a red solid product (45.6 mg, yield: 35.2%).

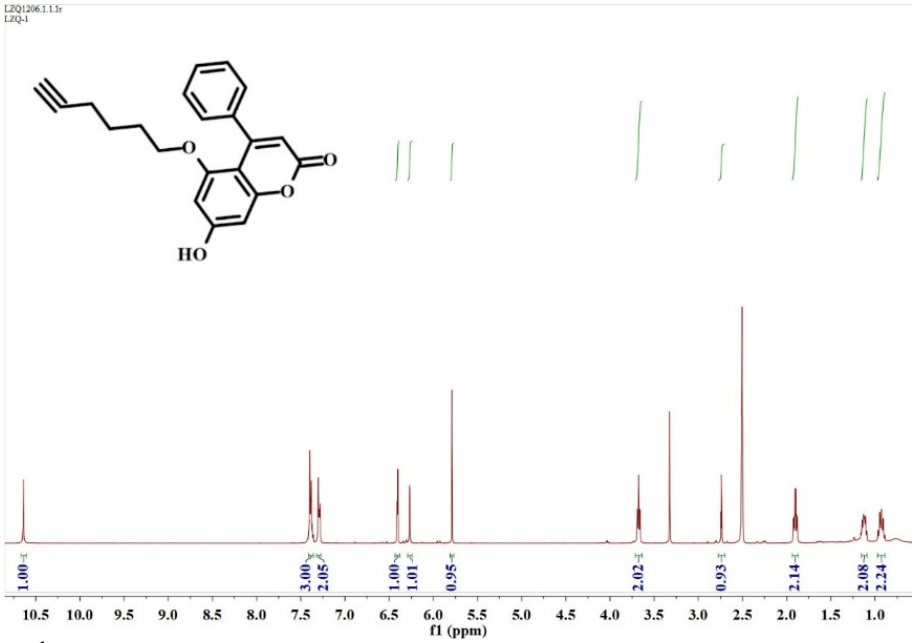

FigureS8. ^{1}H NMR spectrum of alk-DP.

Preparation of azi-TPP ((3-Azidopropyl)triphenylphosphonium Bromide) MS m/z (ESI): 346.4

React (3-bromopropyl) triphenyl phosphonium bromide with 2 equiv of sodium azide and 0.01 equiv of tetrabutylammonium hydrogen sulfate in water at 80 °C. after that, remove the water under vacuum until white crystals precipitate. Finally, filter these crystals and dry under vacuum to obtain azi-TPP (yield: 82.2%).

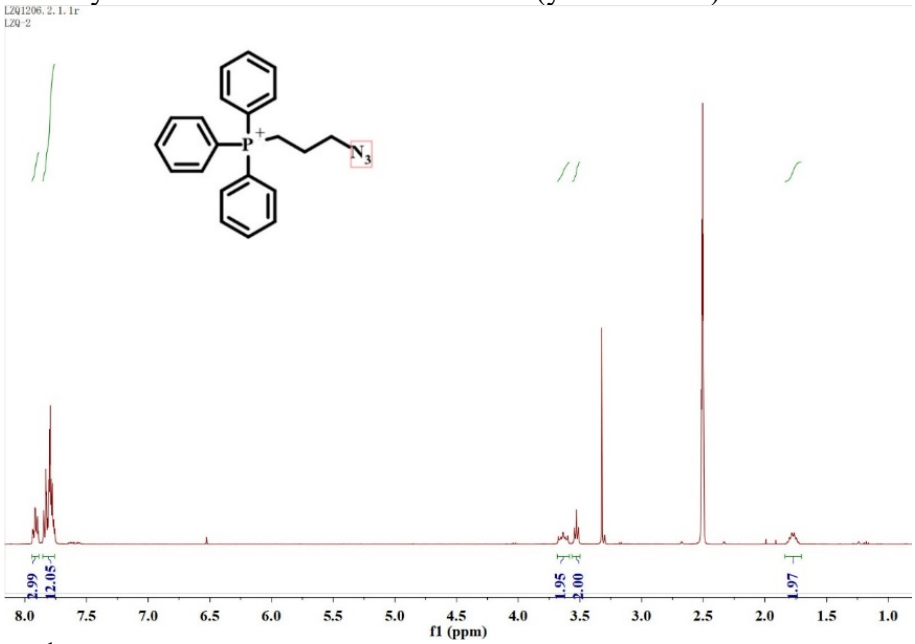

Figure S9. ^{1}H NMR spectrum of azi-TPP.

Preparation of mito-ATTEC MS m/z (ESI): 680.8
A mixture of alk-DP (7.1 mg, 0.02 mmol), azi-TPP (9.2mg, 0.02 mmol), $CuSO_4$ (3 mg, 0.02 mmol), sodium ascorbate (12 mg, 0.06 mmol), H_2O (1 mL) in CH_3OH (1 mL) were stirred in a round bottom flask for 5 hours at room temperature, under argon. The reaction was quenched by water and the mixture was washed twice to afford the desired product (10.2mg, yield: 75%).

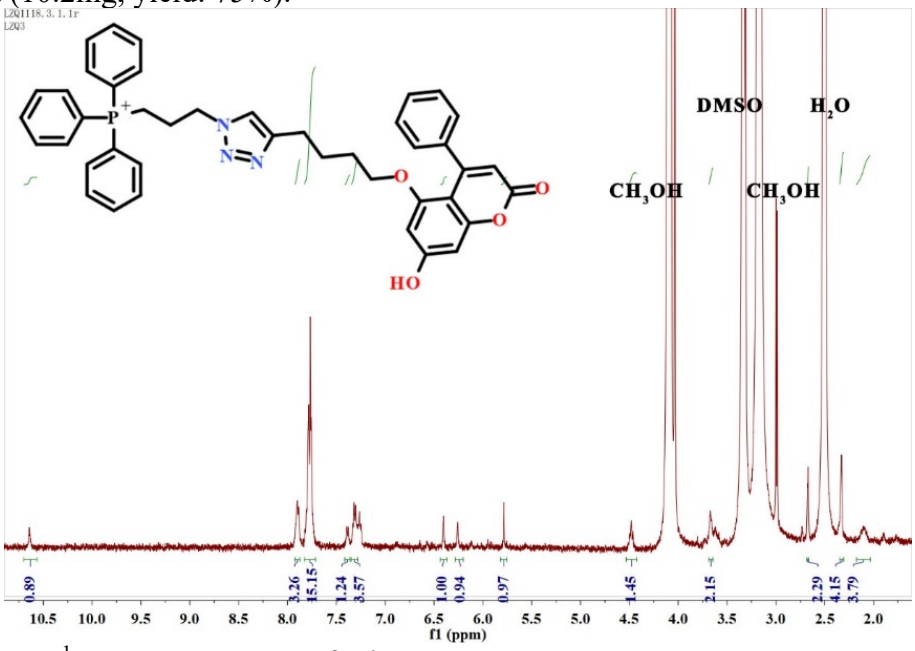

Figure S10. ^{1}H NMR spectrum of mito-ATTEC.

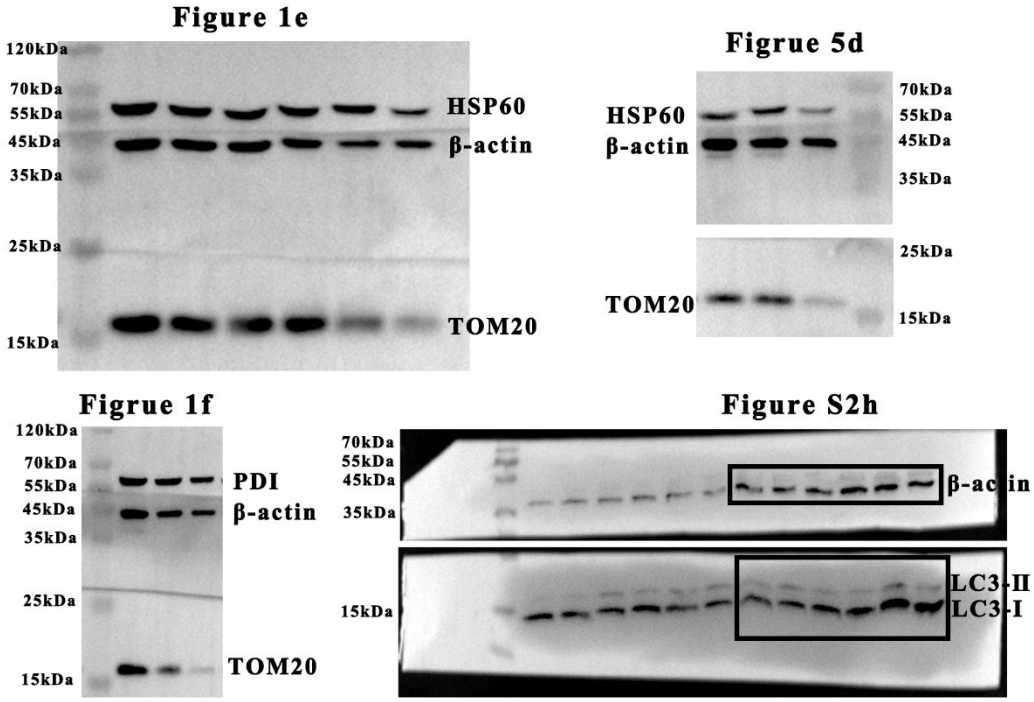

Figure S11. The respective original western blot images